Axial Magnetic Field Lens with Permanent Magnet

Yoshihisa Iwashita
Accelerator Laboratory
Nuclear Science Research Facility
Institute for Chemical Research, Kyoto University
Gokanosho Uji, Kyoto 611, JAPAN

Abstract

A compact Permanent Magnet Symmetric (PMS) lens which produces the axial magnetic field is studied. The proposed lens has no iron pole piece except for the return poles on both ends. It can produce the magnetic field on the axis more than the remanent field of the magnet material by the perpendicular field superimposition.

I. INTRODUCTION

A 7-MeV proton linac was constructed at Institute for Chemical Research, Kyoto University.[1,2] The linac is consisting of a 2-MeV RFQ linac and a 7-MeV Alvarez (DTL). The operating frequency is 433.3 MHz and the structure dimension is compact. Because of the poor vacuum property of the RFQ cavity, two evacuation ports are located at both the entrance and exit side of the cavity.

In order to match the RFQ acceptance, the input beam has to be focused strongly to the RFQ. Unfortunately, the entrance side of the RFQ is occupied by the vacuum port and the final focus element has to be installed into the hole in the end plate of the RFQ. The hole has diameter of 40 mm and the depth of 60 mm. A compact focusing device which can fit in this size had to be devised.

For future study of the simultaneous acceleration of both positive and negative ions, einzel lenses are not preferable. The RFQ requires the round beam in X-Y plane at the entrance, and the quadrupole lenses are not adequate in this respect. A magnetic lens which produces the magnetic field of axial symmetry was picked up as a candidate for the purpose. The field can be produced by a "solenoid". Applications of anisotropic magnet have been studied for charged particle beam manipulations [3,4,5]. With a careful study of the radially oriented anisotropic magnets, it was found that a compact strong Permanent Magnet Symmetric (PMS) lens can be fabricated in the limited size by application of the perpendicular field superimposition.

II. PERPENDICULAR FIELD SUPERIMPOSITION

Let us consider the anisotropic magnet configuration in the two dimensional space as shown in Figure 1. The magnetic field has the direction of Z, and the maximum at the center. The analytical expression for the maximum field is calculated as follows;

$$B_{\max} = \frac{Br}{\pi}\left\{\log\left(1+\frac{l^2}{b^2}\right)-\log\left(1+\frac{l^2}{r^2}\right)\right\}. \qquad (1)$$

0-7803-1203-1/93$03.00 © 1993 IEEE

It can be shown that the value is not finite when $l/b \to \infty$ keeping l/r finite. Because the produced field is perpendicular to the easy axis of the magnet, the operating point in the B-H curve will stay in the upper half. If the magnet material has no knee in the second quadrant of the B-H curve, which is easy requirement for almost rare earth magnet materials, no demagnetization is expected. Although it is only a logarithmic increase, it seems to have no limitation.

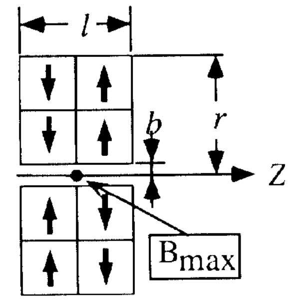

Figure 1. Geometry for field concentration test.

The field concentration by perpendicular filed superimposition is verified by a rough experiment. Eight pieces of 10 mm x 10 mm x 30 mm magnets made of NEOMAX 35H, which has Br of 1.1 [T], are placed as shown in Figure 1. One block is consisted of four pieces which attract each other. Two of the blocks are fixed on jaws of a vice which is made of iron, and put close by pressing with the vice to the gap of 2 mm. The maximum field is measured by an axial Hall probe as 1.6 [T] which is more than Br.

Neglecting the second term of the equation (1) and substituting the values for l and b, we get B_{max}=1.6 [T]. Because the jaws of vice is made of iron, it acts like return yoke. The magnetic field produced by the magnets with the iron return yoke is also calculated by PANDIRA [6]. It also shows the value 1.6[T] as a maximum.

III. PROPERTY OF MAGNETIC FIELD LENS

The focal strength $1/f$ for charged particles with the energy of eV in a magnetic field lens of axial symmetry is given by

$$\frac{1}{f} = \frac{e}{8m_0V^*}\int_{-\infty}^{\infty}B^2dz \quad [\mathrm{m}], \qquad V^* = V\left(1+\frac{|eV|}{2m_0c^2}\right), \qquad (2)$$

where e and m_0 are the charge and the mass of the particles at rest respectively.[7] It should be noted that the focal strength is proportional to B^2 and 20% increase in the focal strength will be obtained by 10% increase of the remanent field which will be achieved by material developments. The drawback is that the temperature coefficient of the focal strength is twice as large as that of the remanent field. On the other hand, this property can also be used as a focal strength adjustment by means of the temperature control. The typical temperature coefficient of the Nd-B-Fe magnet is 0.1% / °C.

IV. MAGNETIC FIELD PRODUCED BY A RADIALLY MAGNETIZED MAGNET

Let us consider a radially oriented permanent magnet ring as shown in Figure 2.

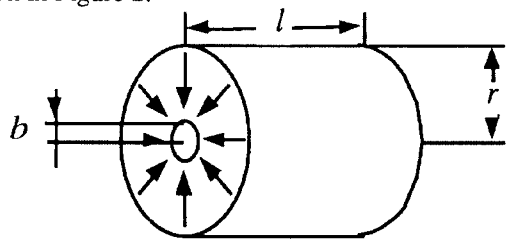

Figure 2. Radially oriented permanent magnet ring

Integrating over the magnetic dipole, the magnetic field on the axis of the magnet is given as

$$B(z)=\frac{Br}{2}\left\{\frac{1}{r_l}-\frac{1}{b_l}-\frac{1}{r_0}+\frac{1}{b_0}+\log\frac{(1+r_0)(1+b_l)}{(1+b_0)(1+r_l)}\right\},$$

$$r_0=\sqrt{1+\left(\frac{z}{r}\right)^2},\ b_0=\sqrt{1+\left(\frac{z}{b}\right)^2},$$

$$r_l=\sqrt{1+\left(\frac{z+l}{r}\right)^2},\ b_l=\sqrt{1+\left(\frac{z+l}{b}\right)^2} \quad (3)$$

The magnetic field has a maximum at z=0, where the end of the magnet is located. The value is

$$B(0)=\frac{Br}{2}\left\{\frac{r}{\sqrt{r^2+l^2}}-\frac{b}{\sqrt{b^2+l^2}}+\log\frac{1+\sqrt{1+l^2/b^2}}{1+\sqrt{1+l^2/r^2}}\right\}. \quad (4)$$

Again, it can be shown that the logarithm term is not finite if keeping l/r finite, and $l/b \to \infty$. In the real applications, two kinds of rings with different magnetization will be placed alternatively. In the case, the magnetic field should be superimposed and the maximum field is doubled. The principle of the perpendicular field superimposition should work here again. For example, a lens of two rings (b=5 mm, r=2 cm, and l=2x2 cm) has the maximum field of 1.22 Br.

V. PMS LENS

To fabricate the real magnet, one has to consider several constraints. The ring should be segmented to realize the radially oriented anisotropic property. The return iron yoke has to be located around the magnet to reduce the leakage field on the axis particularly to the RFQ side. The case of the magnet can be made of iron, and acts as the return yoke. The corners of the magnets are rounded so that the lens has less aberration. The bore hole of the iron case at entrance side is made large to accept a beam with large diameter. The magnet material is NEOMAX 40 which has the remanent field Br of 1.29 T nominal. The final dimensions are shown in Table 1. Photo 1 shows the assembled PMS lens.

The field calculated by PANDIRA is shown in Figure 3. Figure 4 show the magnetic field distribution plots on the axis both the calculated value by PANDIRA and the measured value. The measured peak value is about 10 % smaller than the calculated one. There are three reasons that can decrease the field. 1) The azimuthal segmentation reduces the field. 2) Because of the repulsive force and the tolerances, the bore radius is larger than the designed value. 3) Because of the surface finish for Ni plating on the magnet, the corners of the magnet are rounded. It makes the effective bore radius larger. According to the PANDIRA calculation, 2 % increase of the bore radius will result the 1 % magnetic field decrease. The first one is thought to be the main factor in our model magnet case.

number of ring	2	
outer radius of a ring magnet	17	mm
length of a ring magnet	25	mm
number of segments in a ring	16	
bore radius	5	mm
corner radius of a segment	8	mm
outer radius of iron case	20	mm
length of iron case	60	mm
corner radius and thickness of lids	3	mm
bore radius of entrance lid	7.5	mm
remanent field	1.29	T

Table 1. Model PMS dimensions

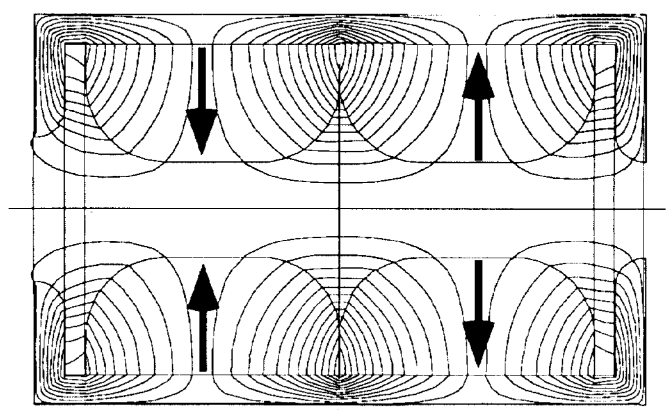

Figure 3. PANDIRA result

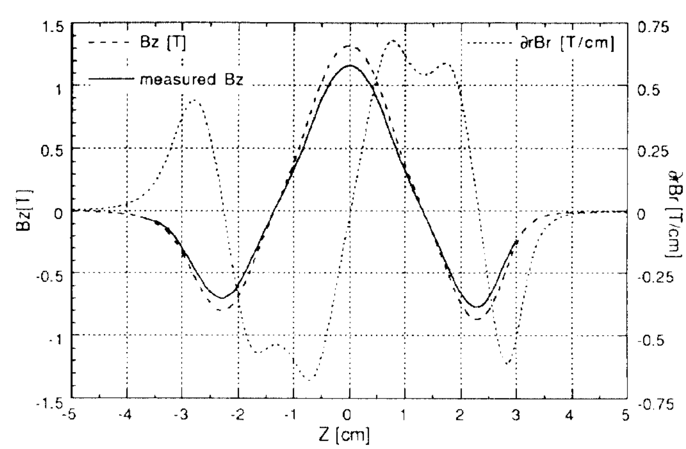

Figure 4. Magnetic field distribution

VI. BEAM OPTICS

The beam dynamics simulations based on the calculated magnetic field distribution by PANDIRA are performed. The equations of motion in the cylindrical coordinate are

$$\begin{cases} m_0\,\dot{v}_r = -q\,v_\theta\,B_z + m_0\,{v_\theta}^2/r, \\ m_0\,\dot{v}_\theta = -q\left(v_z\,B_r - v_r\,B_z\right) - m_0\,v_r\,v_\theta/r \end{cases} \tag{5}$$

The equations are integrated numerically. For less aberration, the r dependence of B_Z and $\partial r B_r$ should be small. One typical result is shown in Figure 5. B_Z and $\partial r B_r$ at 10 different radii are shown on the Z axis. The parallel beams on the x axis with 0.4 mm equally spaced radii start at z=-6 cm (left edge), and go through the PMS whose center is located at z=0. The x-x' phase space plots are also shown at the initial point and the focal point calculated by equation (2). Because the integral over B_Z on axis of PMS lens is zero, the image does not rotate. In this calculation, the space charge is not included yet. Further study will include the space charge effect.

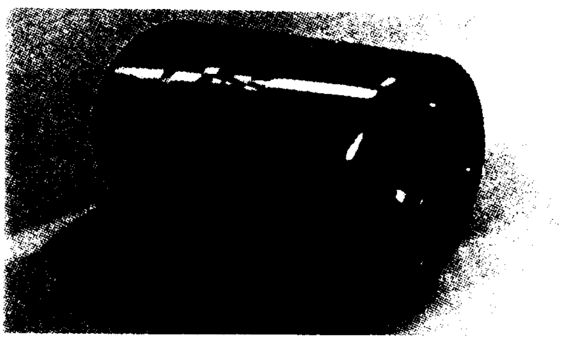

Photo. The assembled PMS lens

VII. ACKNOWLEDGMENT

The author would like to thank R. A. Jameson for the useful information. The model magnet was fabricated by Sumitomo Special Metal Co. LTD.

VIII. REFERENCES

[1] Y. Iwashita, et. al."7MeV PROTON LINAC", Proc. 1990 Linear Accel. Conf., Albuquerque, p.74
[2] A. Noda, et. al. "Improvement of the Proton Accelerator System", Bull. Inst. Chem. Res. Kyoto Univ. Vol.70, No.1 (1992)
[3] O. C. Dermois, "The external injection system for the Groningen cyclotron", Proc. Fifth Int. Cyclotron Conf. Oxford, 620 (1969)
[4] K. Halbach, "Physical and Optical Properties of Rare Earth Cobalt Magnets", Nucl. Instr. and Meth., 109 (1981)
[5] K. Halbach, "Magnet Innovations for Linacs", Proc. 1986 Linac Conf., Stanford, SLAC-Report-303, 407 (1986)
[6] User's Guide for the POISSON/SUPERFISH group of codes., LA-UR-87-115, LANL (1987)
[7] C. Fert and P. Durandeu, "Magnetic Electron Lenses" in "Focusing of Charged Particles", Edited by A. Septier; Academic Press, 309 (1967)

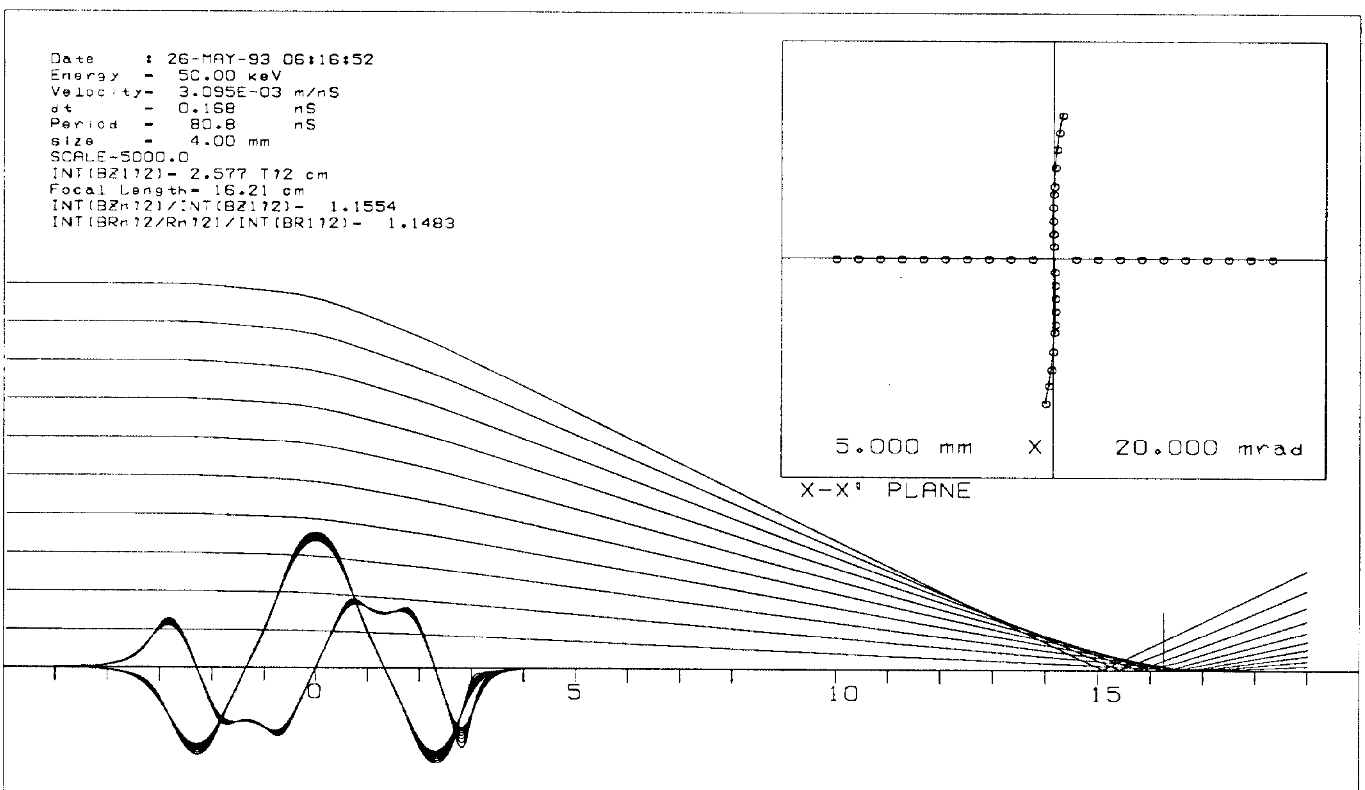

Fig 5. Beam dynamics simulation based on PANDIRA result.